



Contents lists available at ScienceDirect

Journal of Photochemistry and Photobiology A: Chemistry

journal homepage: www.elsevier.com/locate/jphotochem

Effects of sintering of TiO₂ particles on the mechanisms of photocatalytic degradation of organic molecules in water

Timothy Hathway, William S. Jenks*

Department of Chemistry, Iowa State University, Ames, IA 50011-3111, United States

ARTICLE INFO

Article history:

Received 19 May 2008

Received in revised form 11 July 2008

Accepted 16 July 2008

Available online 31 July 2008

Keywords:

Titanium dioxide

Annealing

Photocatalysis

Degradation

ABSTRACT

Partial degradations of 4-methoxyresorcinol and *p*-anisyl-1-neopentyl alcohol were carried out with the PC series of photocatalysts from Millenium Chemicals and with Degussa P25. The PC series of anatase catalysts varies only in the degree of sintering, and thus particle size and type of crystal defects. The initial product distributions were not substantially sensitive to catalyst, implying that none of the major products depended on particular binding sites that could be annealed away. Rate constants varied from catalyst to catalyst, but not dramatically, on a weight-to-volume basis. Thus there was also not a direct connection between available surface area and the rate of degradation. The product distribution as a function of suspension pH is also discussed.

© 2008 Elsevier B.V. All rights reserved.

1. Introduction

Titanium dioxide has been given considerable attention as a degradative photocatalyst in both air and water due to its exceptional ability to decompose organic molecules having a multitude of functionalities [1–4]. Despite the enormous potential of this method, there are two major limiting factors: the lack of absorption of significant portions of the visible spectrum (meaning that solar irradiation is used inefficiently), and the low efficiency of photons that are absorbed. At least in part due to these limitations, photocatalytic degradation of organic compounds in water currently remains in limited use. Research on extending the useful range of light absorption by the catalysts is extremely active, but beyond the scope of this paper. Instead, we now focus on how the properties of a set of closely related catalysts affect the efficiency and chemistry induced by the catalysts. Our approach is to use the well-established chemistry of certain organic probe molecules to report on the effects of the structural variation of the catalyst. Because “home-made” catalysts are subject to subtle reproducibility issues, we take this approach first with a series of commercially available catalysts: the PC series of materials from Millenium Chemicals. Surface area and defect concentration are the largest variables within this series. Recent work by Nowotny et al. points out explicitly, in trying to understand the effects of defects in both undoped and

doped TiO₂-based photocatalysts [5], that detailed characterization of defect type is critical to predicting defect behavior. In the absence of atomic-scale understanding of the defect structure, a strong implication for reproducible results is that comparisons of such effects are best carried out with a standard set of materials whose members are subject to minimal processing differences and are widely available.

The catalysts in the Millenium PC series all derive from PC 500, which is an anatase TiO₂ catalyst with 5–10 nm particle size. Its name correlates with the approximate surface area of the material, as seen in Table 1. The rest of the catalysts in the series are produced by sintering PC 500, causing larger particles to be formed and greater crystallinity within the particles. We also include the industry standard Degussa P25 catalyst in our experiments, for comparison.

In optimizing the conditions for degradation, it has been shown multiple times that the recombination of the two charge carriers, electrons (e⁻) and holes (h⁺), is the major cause of low degradation efficiency in titania [6]. Simply put, electron–hole recombination competes with the ability of the holes either to directly oxidize organic species or to cause hydroxyl-radical-like chemistry.

Sintering affects these dynamics. The greater particle size induced by sintering stems from the merging of smaller particles and crystal annealing. This lowers the number of large-scale surface defects (boundaries, shear planes, etc.) and some small-scale defects (islands, vacancies, etc.). Reduction in defects in turn increases the h⁺ lifetimes by slowing recombination. Thus, the fraction of h⁺ that achieves useful chemistry should increase. At the

* Corresponding author.

E-mail address: wjenks@iastate.edu (W.S. Jenks).

Table 1
Physical characteristics of TiO₂ photocatalysts

Catalyst	Surface area (BET) (m ² /g)	Average particle size (nm)
PC 10	11	75
PC 50	50	25
PC 100	87	20
PC 500	335	8
P25	55	35

same time, sintering can increase surface electron trapping sites (Ti³⁺ centers and oxygen vacancies) [6]. Such centers can increase the average charge separation distance by localizing e⁻ if they are in the bulk of the crystal, but surface traps can again induce recombination. The latter effect is ameliorated by electron scavengers like O₂. Additionally, O₂ can help lead to surface hydroxyl formation on anatase [7–9]. In short, it is probably an oversimplification to say that sintering universally reduces the number of defect sites, but it is generally accepted that it minimizes the types of defect sites that are most damaging to photonic efficiency in the process of particle merger and crystal annealing [6,10,11].

Table 1 shows the effects of sintering PC 500 on the average particle size, which is of the order of 10 nm diameter in the originally prepared material. On the assumption that the rate of a given photocatalytic degradation step is affected by photon flux, available surface for adsorption, and the efficiency of recombination, sintering should lead to opposite-trending effects: slowing down the observed rate because of lower surface area, and raising the observed rate because of fewer recombination sites. Indeed, Pichat has carried out experiments testing just these ideas using several probes and identified varying trends, depending on the substrate [12–14]. Here, we expand on this notion by exploring the type of reactivity observed in addition to the simple rates. The essential hypothesis to test is whether the reduced number of “defects” also affects the type of chemistry (single-electron-transfer based or hydroxyl-like), i.e., whether surface defects (steps, vacancies, etc.) represent sites for preferred types of photocatalytic reactions, in addition to being traps for recombination. We use the previously studied compounds methoxyresorcinol (MR) [15] and 1-*p*-anisyl neopentanol (AN) [16] to carry this out.

2. Experimental

2.1. Materials

All chemicals were obtained from Fisher or Aldrich in the highest purity available and used as received. 4-Methoxyresorcinol (4-methoxybenzene-1,3-diol, MR) [17] and *para*-anisyl-1-neopentanol (AN) [18,19] were prepared by reported methods. *p*-Anisyl *t*-butyl ketone (**8**) was prepared as described by Smyth and Corby [19] reduced with NaBH₄ to produce AN [16]. Compounds **9–11** were commercially available, and compounds obtained from degradation of MR were obtained as previously described [15].

p-Hydroxyphenyl *t*-butyl ketone (**12**) was prepared by demethylation of **8** with thiophenol [20]. Yield 16%, unoptimized. ¹H NMR (CDCl₃, 300 MHz) δ 1.35 (s, 9H), 6.82 (d, *J*=9 Hz, 2H), 7.79 (d, *J*=9 Hz, 2H); ¹³C NMR (CDCl₃, 300 MHz) δ 28, 44, 115, 129, 131, 160, 208, MS (*m/z*) 178 (M⁺), 121 (100), 95, 77, 65. MS (*m/z*) 178 (M⁺), 121, 95, 77, 65.

1-*p*-Hydroxyphenyl-1-neopentyl alcohol (**6**) was prepared by reduction of **12**. Methanol (10 mL) was charged with 1 mmol ketone and stirred while cooling in an ice bath. NaBH₄ (3 mmol) was slowly added and the solution was allowed to warm to room temperature. The mixture was then heated to 70 °C for 5 min and allowed to cool to room temperature, followed by quenching with 10 mL ice water.

The mixture was evaporated under reduced pressure to remove methanol, then extracted with 3 × 15 mL Et₂O, washed with 30 mL brine, and dried over Na₂SO₄. The solvent was evaporated under reduced pressure and the crude solid product was collected without further purification. ¹H NMR (CDCl₃, 300 MHz) δ 0.88 (s, 9H), 4.33 (d, *J*=3 Hz, 1H), 4.72 (s, 1H), 6.76 (d, *J*=8 Hz, 2H), 7.16 (d, *J*=8 Hz, 2H); ¹³C NMR (CD₃OD, 300 MHz) δ 29, 39, 86, 118, 133, 137, 166; MS (*m/z*) 180 (M⁺), 123 (100), 95, 77, 65. MS (*m/z*) 180 (M⁺), 123, 95, 77, 65.

The water had a resistivity of ≥18 MΩ cm⁻¹. Titania samples were the PC series from Millenium Chemical and P25 from Degussa.

2.2. Suspensions and photolyses

The standard suspensions for photocatalytic reactions were prepared to result in 100 mg TiO₂ per 100 mL deionized water. A stock 10 × TiO₂ suspension was added to approximately 80 mL water. Sonication for 5 min was used to break up larger aggregates of TiO₂. As noted, the pH was either not adjusted or set to 2.0 (0.01 M HCl), 8.5 ± 0.5 (0.1 M NaOH added during the reaction as needed), or 12.0 (0.01 M NaOH). Unadjusted suspensions had an initial pH of 4.5–5.5, depending on the catalyst. A stock 10 × aqueous solution of the organic material was added to bring the final organic concentration to 0.3–1.0 mM, and the total volume was brought to 100 mL as necessary with water. The mixture was then purged with O₂ and stirred for 20 min in the dark before the irradiation was started. Both stirring and O₂ purging were continued throughout the reaction. Except as noted, all degradation product identities were confirmed by comparison to authentic samples.

Photocatalytic degradations were carried out with stirring at ambient temperature using a modified Rayonet mini-reactor equipped with a fan and 4 W broadly emitting 350 nm “black light” fluorescent tubes. The number of bulbs ranged from two to eight depending on the desired reaction rate. Ferrioxalate actinometry [21,22] was performed to allow semiquantitative comparison of data obtained from reactions using different numbers of bulbs. Reaction times were dependent on the degree of degradation required.

After appropriate irradiation times, samples were removed and acidified with Amberlite IR-120 ion exchange resin. The TiO₂ was separated by centrifugation, followed by filtration through a syringe-mounted 0.2 μm PES filter. Sample sizes were 1 mL for kinetics or 50 mL for product studies. The latter, larger samples were concentrated by rotary evaporation to approximately 2 mL and the residual water was removed by lyophilization.

Dried samples deriving from methoxyresorcinol were exhaustively silylated by treatment with 1 mL anhydrous pyridine, 0.2 mL of 1,1,1,3,3,3-hexamethyldisilazane (HMDS) and 0.1 mL of chlorotrimethylsilane [23]. Samples were vigorously shaken for 1 min, and allowed to stand 5 min at ambient temperature. The resulting pyridinium chloride precipitate was separated by centrifugation prior to chromatographic analysis. Samples deriving from anisyl neopentanol were dissolved in 0.50 mL of a stock solution of methanol containing a known concentration of dodecane as an internal standard and used directly for chromatographic analysis.

GC–MS work was done with a standard 25 m DB-5 (5% phenyl) column for chromatography, coupled to a time-of-flight mass spectral detector. The temperature program was 130 °C for 2 min, followed by a ramp to 280 °C at 20 °C/min. Routine GC work was done on another instrument with an FID detector.

Kinetic data were obtained using HPLC (diode array UV–vis detection) analysis of 1 mL aliquots that were acidified and centrifuged before injection. A standard C18 reverse-phase column was used. Eluents were 3:7 (v/v) water:acetonitrile for AN-derived reactions and 4:1 v/v mixture of a water and methanol

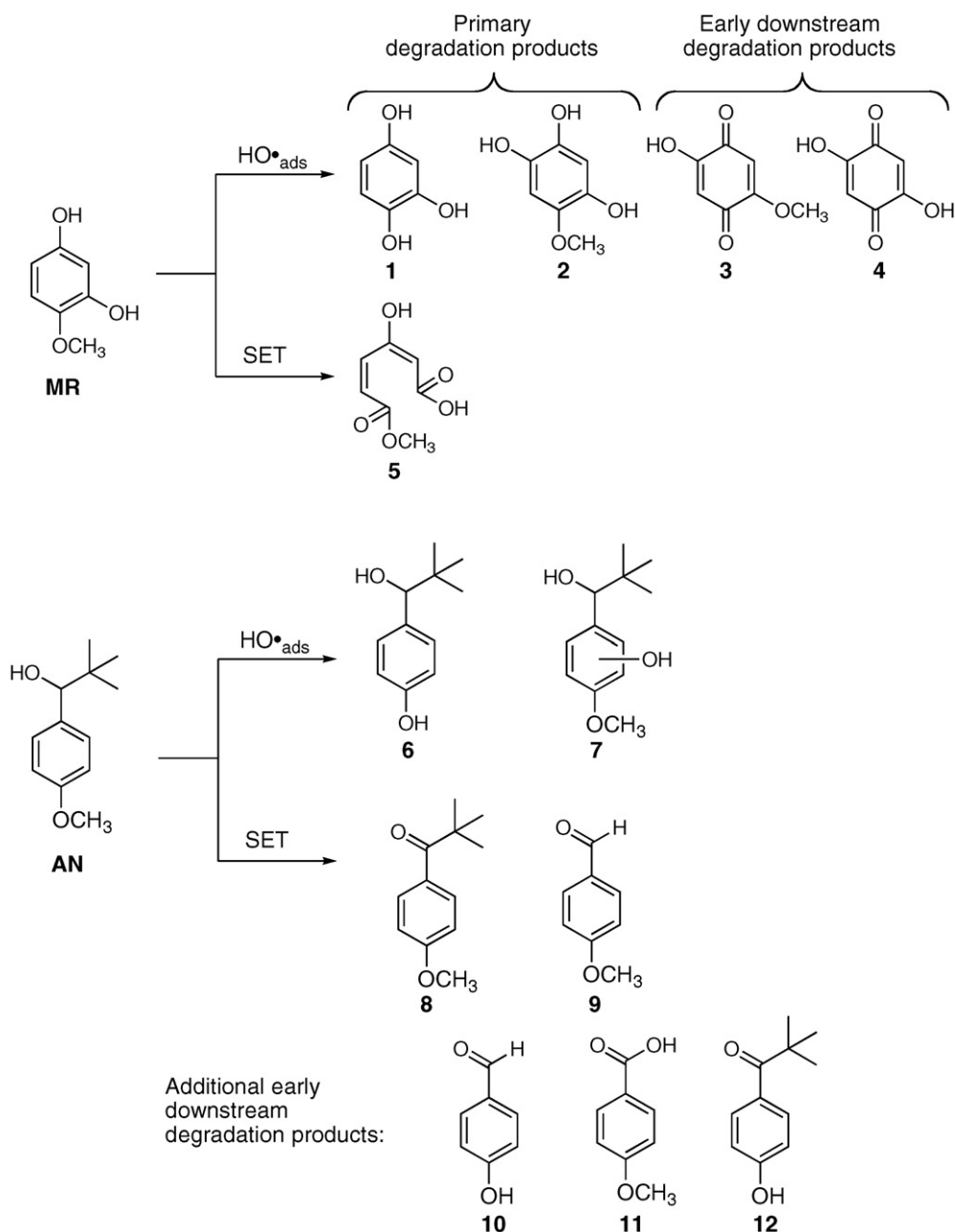
that contained 0.15% acetic acid for the MR runs. Flow was 1.0 mL/min.

2.3. Adsorption

Adsorption equilibrium measurements of MR and AN on P25 TiO₂ were obtained. Suspensions were prepared from 20 mL buffer containing 50 mg TiO₂. The pH was held at 2.0, 7.0, 8.5, and 12.0 using 10 mM phosphate buffer. Unbuffered pH was also used. After allowing the desired contact time, an aliquot was removed, centrifuged and filtered (as above) to remove TiO₂. The residual concentrations were determined by HPLC. Kinetic study showed that the extent of adsorption reached a constant value after no more than 2 h for both compounds. For the quantitative adsorption experiments, at least 20 h equilibration was allowed before measurement.

3. Results

Two probe molecules, MR and AN, were used to examine the series of catalysts for initial rates of decomposition and for product distributions at low conversion. Both MR and AN have previously been documented to show products characteristic of both reactivities attributable to hydroxyl-radical-type chemistry (hereafter referred to as HO_{ads}[•]) and single-electron-transfer (SET) chemistry [15,16]. Proposed mechanisms for these reactions are discussed in these references. MR was chosen from among a series of hydroxylated/methoxylated benzenes because it showed both the HO_{ads}[•] chemistry (hydroxylation and demethylation) and SET chemistry (ring opening), and would thus be a more sensitive reporter molecule than the corresponding trimethoxy- or trihydroxybenzenes, which gave exclusively HO_{ads}[•] or SET chemistry, respectively, with P25 [15]. These products are illustrated in Scheme 1, along



Scheme 1.

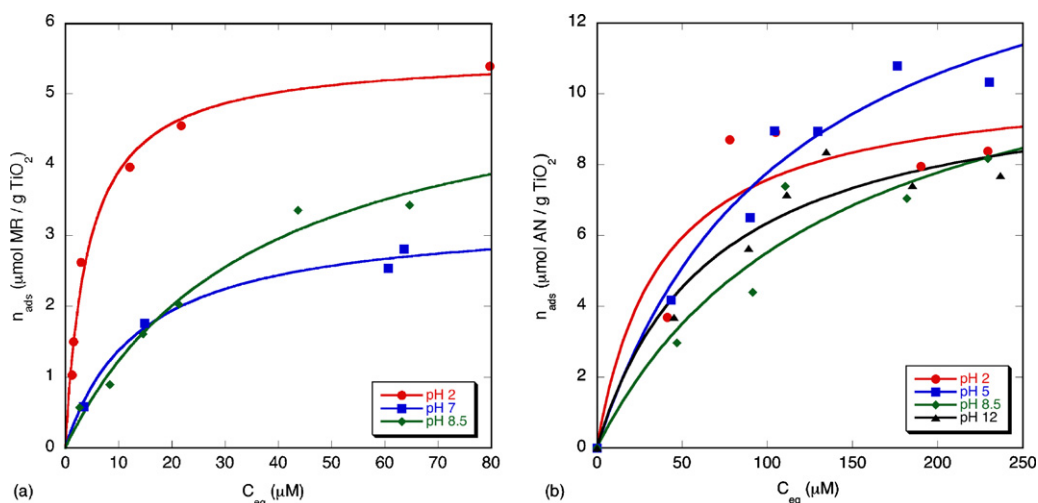


Fig. 1. Adsorption isotherms for P25 (a) MR and (b) AN.

with some additional products that clearly show multiple reaction steps. Because we know that 1,2,4-benzenetriol produces almost exclusively ring opened products [24], we can attribute these secondary hydroxylated and opened products to hydroxylation–first, rather than ring opening–first sequences. After ring opening, subsequent oxidations result in compounds that are easily distinguished as being further downstream by the smaller number of carbon atoms (and hence mass).

AN is expected to have a different binding motif than MR, and also shows different SET chemistry, namely loss of the *t*-butyl group and oxidation to the corresponding aldehyde, as illustrated in Scheme 1 [16]. These were established by analogy to results with homogeneous solution-phase SET reagents [25]. Also illustrated are secondary degradation products, but in this case, it is not as obvious in which order the chemistry occurs.

Ideally, the reactions used to determine product distribution are carried out to very low conversion in order to get the best representation of initial products. Degradation of the early intermediates can be very competitive with or faster than that of the starting material. We presume this is because the more highly oxidized functionality is more adherent to the catalyst, thermodynamically easier to oxidize (e.g., by SET), or both. (The lack of any observed intermediates while degradation is taking place is indicative of this in the extreme limit.) The counterbalance to this desire for low conversion is simply having enough material to characterize. Our experience is that conversion of about 20% of the original material is a good starting point to look for intermediates at reasonable concentrations.

3.1. Adsorption

Dark adsorption isotherms for MR and AN were obtained using P25 at 2.5 g/L. Though the relationship between dark adsorption

and the rate of degradation of compounds is certainly not direct, certain functional groups may exhibit different types of binding under different conditions (e.g., pH), which can result in different interactions with the catalyst surface, and potentially differing reactivity.

Fig. 1 illustrates dark adsorption isotherms for (a) MR and (b) AN, obtained at different pH values. It was found that MR is not stable in highly basic aqueous solutions so isotherms were obtained at pH 2.0, 7.0, and 8.5. The smooth curve is a least squares fit from the Langmuir–Hinshelwood model (Eq. (1)), where the ordinate is the amount adsorbed per gram of catalyst n_{ads} , the abscissa is the equilibrium dissolved concentration of the organic compound (C_{eq}), and K_L is the adsorption equilibrium constant.

$$n_{\text{ads}} = \frac{n_{\text{ads(max)}}K_L C_{\text{eq}}}{1 + K_L C_{\text{eq}}} \quad (1)$$

The curves show a higher capacity of binding (saturation) at low pH for MR. For AN, the data are not as clear, and unfortunately cannot be made much better because 250 μM is nearing the limiting solubility point. Linearization by inversion of Eq. (1) [26] and fitting the data result in capacities and binding constants given in Table 2. The errors are taken as standard errors of the linear fit propagated through the equations. Despite the variation in the binding constants and adsorption capacities, these data and Eq. (1) can be used to show that all of the degradation experiments were carried out under conditions where the catalyst is saturated, yet only a relatively small fraction of the MR or AN is bound to the catalyst surface at any given moment [27].

MR, which has easily deprotonated phenolic sites, shows a fairly dramatic change in binding constant with pH. It is well known that carboxylic acids also are stronger binders to TiO_2 at low pH; we take this to be an example of an analogous phenomenon.

Table 2
Adsorption isotherm data for MR and AN in the presence of 2.5 g/L P25 TiO_2

Probe molecule	pH	Adsorption capacity ($\mu\text{mol/g}$) ($n_{\text{ads,max}}$)	Adsorption capacity (molecules/nm^2)	Binding constant (K_L , mM^{-1})
MR	2	14.2 ± 0.2	0.156 ± 0.002	205 ± 20
	7.0	8.3 ± 0.6	0.091 ± 0.007	66 ± 15
	8.5	18 ± 2	0.20 ± 0.02	19 ± 2
AN	2	25 ± 5	0.28 ± 0.06	28 ± 22
	5	41 ± 7	0.45 ± 0.08	9 ± 2
	8.5	35 ± 11	0.39 ± 0.12	6 ± 2
	12	25 ± 4	0.28 ± 0.04	16 ± 16

Table 3
Initial rates of loss of MR and AN with equal mass catalyst

Compound	Catalyst	Degradation rate ^a : Absolute rate ($\mu\text{M}/\text{min}$) and rate normalized for catalyst surface area ($\text{nM g}/\text{m}^2 \text{ g}$)			
		pH 2	Unbuffered ^b	pH 8.5	pH 12
MR ^c	PC 10	1.0 (94)	0.6 (53)	22 (2000)	^d
	PC 50	1.0 (20)	1.0 (20)	36 (774)	
	PC 100	0.9 (10)	1.1 (13)	48 (554)	
	PC 500	0.3 (1)	0.04 (<1)	12 (56)	
	P25	1.2 (22)	1.0 (18)	28 (502)	
AN ^e	PC 10	7 (650)	13 (1200)	9 (850)	10 (900)
	PC 50	16 (320)	12 (240)	14 (270)	16 (330)
	PC 100	24 (280)	6 (73)	11 (120)	9 (100)
	PC 500	12 (36)	4 (11)	5 (16)	7 (20)
	P25	30 (550)	30 (540)	9 (160)	19 (340)

^a Standard errors of fits from linear plots were almost all approximately 10% or less.

^b pH approximately 5.0 ± 0.5 .

^c Initial concentration 2.0 mM.

^d Not measured due to base hydrolysis.

^e Initial concentration 0.30 mM. Rates at pH 2 and unbuffered pH were obtained with higher lamp intensity and normalized to the other rate constants by means of ferrioxalate actinometry.

By contrast, the binding constants measured for AN (which are subject to considerably larger error) were arguably invariant to pH, and certainly do not show a clear trend as do those for MR. Though the charge on the TiO_2 surface clearly still varies with pH (its *pI* being routinely quoted from 4 to 6, depending on material), the hindered alcohol in AN undoubtedly has a pK_a outside the range examined here, probably in the range of 16–18.

3.2. Initial degradation kinetics

Photocatalytic degradation usually follow apparent first order kinetics. However, the initial kinetics (e.g., to 20–30%) can be reasonably approximated to the more traditional zero-order kinetics for photochemical reactions. Either approach can be valid, depending on the range of interest. Since we were interested in the initial chemistry, we obtained zero-order rate constants for the early-phase degradation of both probe molecules with the variety of catalysts at several pH values. These are given in Table 3. The absolute rate constants, obtained with initial concentrations of 0.3 mM (AN) or 1.0 mM (MR) depend on lamp intensity, sample geometry, and so on. However, all these parameters are held constant for the series, so the relative values are meaningful.

All samples were prepared with the same density of catalyst on a weight-to-volume basis. Analyzing the data in this way, the catalyst-to-catalyst variation in rate is not large. Unbuffered PC 500 was slower than the rest for both probe molecules, but otherwise, most rates are within a factor of 3 of one another. At low pH, it is possible that the degradation of MR is being artificially lowered by the presence of chloride ions, perhaps by a factor of two, as documented for benzoic acid derivatives [28,29]. However, this does not neither account for the full variability of the rate, nor for the results with AN (below).

Considering the rates as a function of catalyst surface area gives an alternate picture. (Remember that the names of the PC series correspond approximately to the BET surface area in m^2/g . The surface area of P25 is about the same as PC 50.) Notably P25 and PC 50 have fairly similar rates when expressed this way, but it is the larger particles that have the highest rates per surface area on the whole.

The initial degradation rates were sensitive to pH, particularly for MR. The rate of degradation was greatest at pH 8.5, which is also the pH at which the most intermediates are generally observed for molecules of this type [15,24]; this may be because ~ 8.5 is the pH

at which the relative rate of degradation of MR is greatest, relative to the downstream intermediates, causing their apparent accumulation. No reliable data are available at pH 12 due to decomposition of MR in the dark.

For AN, there was considerably less pH sensitivity for PC 10 and PC 50, the most annealed catalysts. For the original catalyst PC 500 and for PC 100, there was a somewhat larger variation: a factor of 2–3 across the pH spectrum with the low rates being the unbuffered case. For P25, the minimum degradation rate was observed at pH 8.5, but it was still within a factor of 3 of the fastest degradations. The initial pH of the unbuffered suspensions was 4.5–5.5, depending on the catalyst.

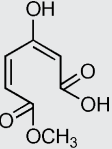
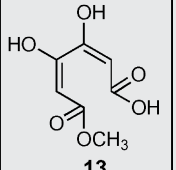
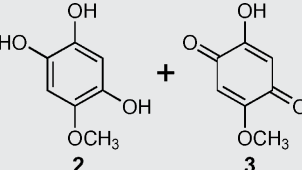
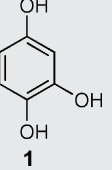
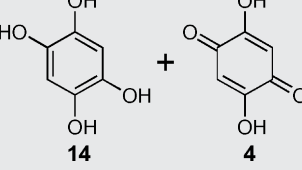
3.3. Product distributions

3.3.1. MR degradations

Degradations were carried out at several pH and catalyst combinations. The product distributions obtained using PC 100 are shown in Table 4. As in our previous work [15], the intermediates were silylated before separation and identification by GC–MS. The tabulation is given in order of short to long retention time of the silylated derivatives by GC. The compounds are illustrated in their form before silylation, and are also drawn as the most obvious tautomer, e.g., **5**. In addition to the compounds illustrated in Table 1, another multiply reacted compound, **13**, was observed. Very qualitative observations on the intensities of the GC peaks are given in Table 4, with the largest peaks being a few percent of that of the remaining starting material. Note that pairs of hydroquinones and quinones are given as a single compound, as they are interchangeable by trivial air oxidation or by reduction by TiO_2 [30]. Very small quantities of 3–5 carbon compounds were also observed, indicating that some intermediates were undergoing successive decomposition steps even at fairly low conversion.

The results in Table 4 were obtained with PC 100, but they are representative of all the other catalysts tested, including P25; qualitatively identical distributions were obtained at equal conversion of the starting material. Compounds **1–5**, and **14** were identified as their silylated derivatives, as previously described [15,24]. Compound **13** is shown in brackets because its structure is only tentative; in fact it is most likely a combination of two or more isomeric structures where MR has been hydroxylated twice and the ring opened. The suggestion that it is a mixture comes from the observation that the GC peak was always broad, relative to the others.

Table 4
Products observed on photocatalytic degradation of MR using PC 100

Compound ^a	Abundance			
	pH 2	pH 5.5 ^b (unbuffered)	pH 8.5	pH 12
 5	-	-	Low	Medium
 13	-	-	Medium	High
 2 + 3	Low	Medium	High	-
 1	Medium	Medium	-	-
 14 + 4	-	-	High	High

^a Compounds are listed in order of GC elution.

^b The initial pH of the unbuffered solution was 5.5 using PC 100 and dropped about 1 pH unit through the photolysis. The pH of the unbuffered solution varied slightly from catalyst to catalyst.

The formula and proposed structural assignment is done by analogy to compounds **48** and **51** from Li et al. [15]. These compounds differ by $m/z=88$, i.e., a $(\text{CH}_3)_3\text{SiO}$ substitution as do **13** and **5**. Characteristic losses of CH_3 , $\text{CO}_2\text{Si}(\text{CH}_3)_3$, and CO_2CH_3 are noted for each compound. The retention time of **13** was the longest of any of these, also consistent with a more substituted compound.

Clearly, multiple steps are required to get to structure **13**. We presume that hydroxylation to **2** is the first step, i.e., $\text{MR} \rightarrow \mathbf{2} \rightarrow \mathbf{13}$. After **2**, the path is more uncertain, and multiple regioisomers are obtained. We speculate that another hydroxylation follows, and ring opening is the third step. The position of the ring opening could also provide multiple isomers. Again, we speculate that cleavage between two *ortho* hydroxyl groups is favored over other positions on the basis of analogy [24,31]; a few of the potential structures for **13** are illustrated in Scheme 2. (Again, these are illustrated as the most suggestive possible tautomer.)

While very similar product distributions were obtained with each catalyst, there was a striking effect of pH on the observed product distributions: under acidic conditions, only demethylation product **1** and hydroxylation products **2** and **3** are detected. Somewhat higher concentrations of the hydroxylation products are seen

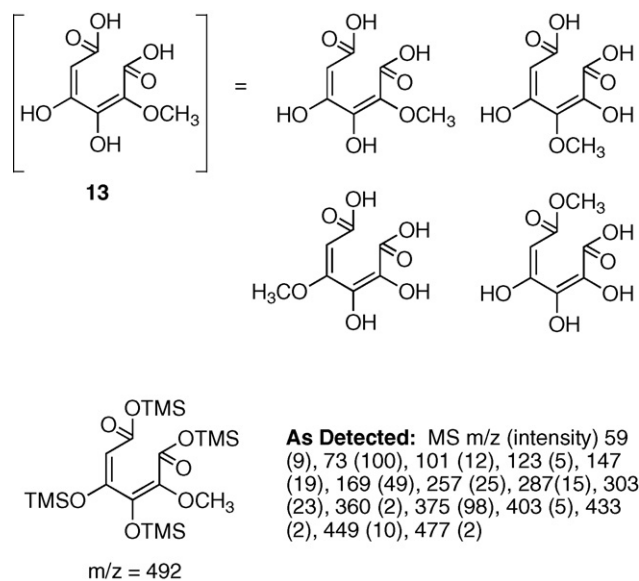
at the still-acidic but higher pH extent when the system is not buffered. At the intermediate pH of 8.5 and at pH 12, both SET and $\text{HO}_{\text{ads}}^{\bullet}$ products are observed.

3.3.2. AN degradations

Degradations of AN were carried out in similar fashion, but the products of these reactions did not require silylation for observation by GC. The results of photolysis, using PC 100 at pH 2, are shown in Table 5. It is at this pH at which the greatest number of intermediates is observed. Product distributions under other conditions are discussed below. We made no attempt to observe *t*-BuOH, *t*-BuOOH or other small alkyl products.

All compounds were identified by comparison to authentic samples, save for **7**. Its structure is proposed from the mass, and we do not know the position of the hydroxylation, but it would ordinarily be favored *ortho* to the methoxy group over being *ortho* to an alkyl substituent. Hydroxylation of the alkyl group was dismissed due to lack of precedent under related oxidative conditions [32,33].

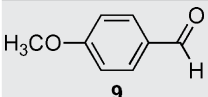
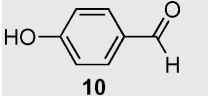
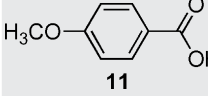
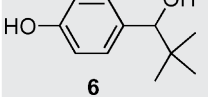
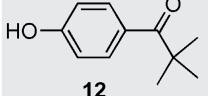
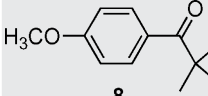
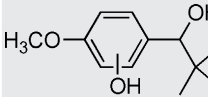
Treatment of AN with chemical SET reagents results in formation of **9** by cleavage of the resulting radical cation [16]. Thus, **9** is taken as a marker for SET chemistry by TiO_2 . Ketone **8** is a substan-



Scheme 2. Potential isomers for compound **13**.

tial product in conventional SET reactions [34], but it is a minor product in Ranchella's titania-in-acetonitrile work, as it is here. Ranchella et al. showed it also to be a marker for SET reactions for TiO₂.

Table 5
Products observed on photocatalytic degradation of AN to low conversion at pH 2 using PC 100

Compound	GC peak size (s/ml)	Retention time (min) ^a	Principle MS peaks, <i>m/z</i> (relative intensity) ^b
 9	Small	3.85	77 (25), 92 (15), 107 (30), 135 (100), 136 (68)
 10	Small	4.47	65 (23), 93 (38), 121 (100), 122 (91)
 11	Small	4.96	77 (5), 96 (5), 121 (10), 122 (9), 135 (12), 151 (100), 152 (9)
 6	Medium	6.11	65 (5), 77 (14), 95 (16), 123 (100), 180 (3)
 12	Small	6.15	65 (8), 93 (9), 121 (100), 178 (4)
 8	Very small	6.30	77 (18), 91 (19), 121 (13), 135 (100), 192 (1)
 7	Medium	6.86	57 (8), 65 (15), 93 (36), 125 (20), 153 (100), 210 (8)

^a The temperature program of column was as follows: initial time of 2 min at 130 °C; ramp from 130 to 280 °C at 20 °C/min.

^b EI-TOF as GC detector.

Compound **6** is an example of the demethylation chemistry that we have shown can come about through either stepwise oxidation of the methyl group or *ipso* attack [35]. We attribute this to HO[•]_{ads}. Again, while SET-based mechanisms can be written down, we attribute hydroxylation of AN to form **7** to HO[•]_{ads} chemistry.

Several of the compounds in Table 5 are clearly secondary products. Demethylation of AN to form **6**, followed by SET oxidation to **10** seems a more likely sequence than the opposite, in that the aldehyde is such an easily functionalized position. At modest conversion, **11** is observed (clearly via aldehyde **9**) but not 4-hydroxybenzoic acid. This lends at least circumstantial support for this proposed sequence of AN to **6–10**. 4-Methoxybenzoic acid (**11**) has been observed previously as a product from AN using organic dyes as SET reagents [34], but not from TiO₂ oxidations. It could also come about through Bayer–Villiger chemistry from peroxides. We believe that **11** is the source of small quantities of anisole that can be observed when the conversion of AN is taken as high as 50%. This is attributed to standard photo-Kolbe type chemistry, and is a standard SET reaction of carboxylic acids.

Another secondary product is ketophenol **12**. Whether it is formed via **6** or **8** cannot be determined; both are possible and both may occur.

Ultimately, the data in Table 5 show that similar quantities of SET and hydroxyl-type products are derived from the initial steps of degradation of AN at pH 2. This is in distinct contrast to the observations at higher pH values. Unbuffered reactions (pH 4.5–5.5) showed nearly a 10:1 ratio of the hydroxylation to SET oxidation products. At any higher pH (8.5 or 12) the SET products were simply undetectable. Again, while we cannot absolutely rule out that the

SET products are degraded more efficiently at high pH, this seems an unlikely explanation. Here, we take into account the ordinary result with carboxylic acid derivatives that their degradation is also faster at low pH. Thus, we at least tentatively conclude that there is a true change in the balance of chemistries, with high pH favoring hydroxylation of AN over SET-induced cleavage. This is in contrast to the case for MR, where more SET-type products are observed at high pH.

4. Discussion

Pichat and coworkers have recently published a trio of papers also evaluating this series of catalysts by measuring the relative rates of degradation of a set of probes, but using a much different set of probe molecules: 4-chlorophenol, 2,5-dichlorophenol, 4-chlorobenzoic acid, dichloroacetic acid, phenol, anisole, and pyridine [12–14]. All of their studies were carried out under unbuffered conditions, presumably near pH 5. Compared to our conditions, differences are that they used a modestly higher catalyst suspension “concentration” and lower organic compound concentration, such that our catalyst loading is somewhat higher (within an order of magnitude). Also, we flush with O₂, while the Pichat’s experiments were carried out under air, so the concentration of O₂ is higher in our experiments. We carried out some control experiments with air bubbling and did not note any discernable differences.

They observed that the phenols, anisole, and 4-chlorobenzoic acid were degraded more rapidly by the catalysts sintered at higher temperature (e.g., PC 10 was faster than PC 500). For pyridine and dichloroacetic acid, the trend was reversed. (PC 10 provided anomalously fast degradation of pyridine.) For most of the compounds, the range of rate constants was within a factor of 4–7, but the rate of degradation of anisole was about 33 times faster using PC 10 than using PC 500 and the fastest catalyst for pyridine (PC 10) was faster by an order of magnitude than the slowest catalyst (PC 50).

Their interpretation focused on the balance between reducing defects in the titania anatase crystals (which are thought to lead to more rapid electron-hole recombination and thus photon wastage) and reducing surface area (which might lead to lower catalytic rates because of less adsorbed material). The reduction of surface area with higher temperature sintering is directly documented for these catalysts (Table 1), and the reduction of crystalline defects is of course completely expected by the sintering/annealing process, if not directly quantified.

Pichat et al. concluded that the drop in rates for dichloroacetic acid and pyridine degradation were attributed to the need for direct adsorption of these compounds to the catalyst in order for “hole attack” (SET) to occur. For the other compounds, it was concluded that direct adsorption was not required, and the lower rate of electron-hole recombination dominated the kinetics. The assumption was that hydroxyl-like chemistry (perhaps literally HO• radicals) could occur in the first few layers of solvent surrounding the catalyst.

We have similarly concluded in previous work that SET chemistry required what we called specific adsorption, whereas hydroxyl-type chemistry did not—and that the latter might happen in the multilayers around the catalyst [15].

Therefore, a study related to the Pichat’s work, in which variable chemistry, i.e., products deriving from differing mechanisms (hydroxyl-like vs. SET) was warranted and might serve to confirm the Pichat hypothesis. We chose these two molecules AN and MR, since both were easily capable of displaying products of both types of chemistry as had been demonstrated in earlier papers. These choices contrast with Pichat’s probes, which generally were molecules that had a strong bias for one type of reactivity or the

other. Like Pichat, we chose to work at least initially (i.e., for this paper) with catalysts that would be available and thus completely reproducible to the full community, i.e., the PC series and P25.

At unbuffered pH, we see little systematic effect among the catalysts. However, on an equal weight-to-volume basis, PC 500 was a less efficient catalyst (factor of ~25) for degradation of MR than the others. The catalyst with the highest surface area and highest defect concentration was thus the slowest catalyst for MR, but the product distribution was not significantly different for this catalyst, compared to the others.

For AN, there was a general downward trend in rate from PC 10 to PC 500 in unbuffered suspensions, but it was not dramatic, only a factor of 3. Again, although smaller, the trend is to higher efficiency at this pH with fewer defects and smaller surface area. The products were invariant with catalyst. While the modest effects on observed rate were in line with the results reported by Pichat and coworkers [13], we thought more specific control of the pH might yield more systematic data.

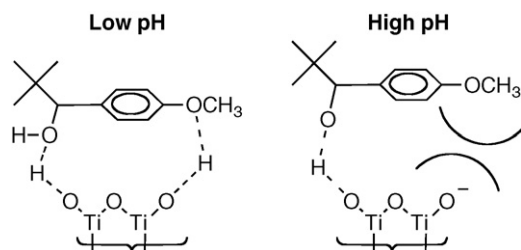
At acidic pH (2.0), we see essentially no difference among the PC series for MR, save for a modest decline (factor of 3) for PC 500. For AN, the rates go up from PC 10 to PC 100 (factor of 3–4) and then fall again for PC 500 (factor of 2). This latter trend of a modest increase in observed rate that peaks for one of the two “middle” catalysts is reproduced for both MR and AN at pH 8.5 and 12.

For any given catalyst, we also do not see a dramatic shift in the reaction rates across pH, with a single exception, which is the high pH degradation of MR. We believe this is attributable to the fact that the pK_a of MR is within a couple of units of 8.5 and that the phenolate should be easier to adsorb and degrade than the phenol. By contrast, if there is any significance to the pH dependence of the rate data for AN, it is in the direction that degradation is somewhat faster in more acidic conditions. A speculative interpretation of the acceleration is probably not justified on the basis of the data in hand.

The product distributions as a function of pH, however, are notably different for both probes. For MR, more ring opening reactions are observed at high pH. Given that we attribute such ring opening reactions to SET chemistry, and that we believe the SET chemistry requires adsorption, we offer the following interpretation.

The strongest adsorption points in MR are clearly the two phenolic groups. However, with the groups positioned *meta* to one another, only one of them may adsorb directly to the TiO₂ surface, and the other is necessarily exposed to the aqueous layers. Certainly by pH 12, and probably at least significantly by pH 8.5, a large fraction of the exposed phenolic hydroxyl groups are deprotonated. These adsorbed phenolates certainly have lower oxidation potentials than their protonated counterparts. Although there is certainly enough chemical potential available from a TiO₂ h⁺ to oxidize any of these species, it has been our experience that there is a qualitative correlation between low oxidation potentials and rapid SET-type chemistry [15,24,31].

For AN, the distinction between low and high pH products is that at higher pH, no SET products are observed, i.e., none of the compounds in which the *t*-butyl group has been removed are found, but hydroxylation and demethylation products are still obtained. A model that might account for this is based on the formation of hydrogen bonds between the *para* methoxy group of AN and the surface of the catalyst, in addition to what we presume is the stronger interaction between the alcohol and the TiO₂ (Scheme 3). At high enough pH, the majority of the surface TiOH groups are not protonated and cannot easily interact with the OCH₃ group. As a result, there may be a tendency for the phenyl group not to be as closely held to the surface. When the interaction is stronger due to the ability of the surface to form hydrogen bonds to the OCH₃



Scheme 3.

at low pH, oxidation of the phenyl ring by SET is facilitated by its proximity to the surface, and the SET-induced chemistry, namely loss of the *t*-butyl group, may occur.

One plausible interpretation of the data presented here is that most of the chemistry, regardless of the conditions, occurs in solution rather than on the surface, and thus hydroxyl-type chemistry predominates for all catalysts: all potential variability attributable to the catalysts is washed out. This may be correct for certain pH conditions, e.g., AN degradations at high pH. However, the very observation of substantial fractions of SET products under other conditions (e.g., AN at low pH and MR at higher pH) belies this as a universal interpretation, as long as it is postulated that SET chemistry demands adsorption. We are not yet prepared to abandon that hypothesis.

5. Conclusions

We draw two conclusions from the observations reported in this paper. If it were the case that degradation reactions, or even particular forms of degradation chemistry, required adsorption to certain types of defect sites, we would expect a strong inverse correlation between the degree of sintering in these catalysts and formation of that class of compounds. It would be the case that on a per gram basis, the absolute concentration of available defect sites would decrease dramatically from PC 500 to PC 10. Thus, product distributions should vary with the catalyst, especially with our relatively high catalyst loading. However, we see no such consistent trend in the data. We can conclude that adsorption to special reactive sites that can be annealed away is not required.

In the second place, we do not find strong evidence to confirm Pichat's hypothesis regarding the effects of sintering on rate. If mutually compensating effects of decreasing surface area and decreasing defect concentration affects the rates of SET. Chemistry in one way (lowering it due to the need for adsorption) and HO[•]_{ads} chemistry the other (raising it, because adsorption is not critical), we would expect to see distinctions in product distributions among the catalysts. Particularly the example of MR at pH 8.5 stands out as having both kinds of chemistry observed for all catalysts, and not in significantly different proportion. The same is true of the degra-

dation of AN at low pH. We do not argue that these experiments disprove the Pichat's hypothesis, but we do not find support here either. From a strictly practical point of view, the effects of differing catalysts among this series are of the same magnitude as those of pH, light intensity, and other experimental parameters, and can be different, even in direction, for different substrates.

Acknowledgment

The authors gratefully acknowledge support from the National Science Foundation (NSF CHE0518586).

References

- [1] P.K.J. Robertson, D.W. Bahnemann, J.M.C. Robertson, F. Wood, Handbook of Environmental Chemistry, vol. 2, 2005, pp. 367–423.
- [2] D. Bahnemann, J. Cunningham, M.A. Fox, E. Pelizzetti, P. Pichat, N. Serpone, in: G.R. Helz, R.G. Zepp, D.G. Crosby (Eds.), Book: Photocatalytic Treatment of Waters, 1994, pp. 261–316.
- [3] W.S. Jenks, in: V.H. Grassian (Ed.), Book: The Organic Chemistry of TiO₂ Photocatalysis of Aromatic Hydrocarbons, CRC Press, Boca Raton, 2005, pp. 307–346.
- [4] P. Pichat, Environ. Sci. Pollut. Control Ser. 26 (2003) 77–119.
- [5] M.K. Nowotny, L.R. Sheppard, T. Bak, J. Nowotny, J. Phys. Chem. C 112 (2008) 5275–5300.
- [6] T.L. Thompson, J. John, T. Yates, J. Phys. Chem. B 109 (2005) 18230–18236.
- [7] M.A. Henderson, W.S. Epling, C.H.F. Peden, C.L. Perkins, J. Phys. Chem. B 107 (2003) 534–545.
- [8] C. Minero, G. Mariella, V. Maurino, E. Pelizzetti, Langmuir 16 (2000) 2632–2641.
- [9] K.I. Hadjiivanov, D.G. Klissurski, Chem. Rev. 25 (1996) 61–69.
- [10] M.R. Hoffmann, S.T. Martin, W. Choi, D.W. Bahnemann, Chem. Rev. 95 (1995) 69–96.
- [11] M.A. Fox, M.T. Dulay, Chem. Rev. 93 (1993) 341–357.
- [12] R. Enriquez, P. Pichat, J. Environ. Sci. Health A 41 (2006) 955–966.
- [13] R. Enriquez, A.G. Agrios, P. Pichat, Catal. Today 120 (2007) 196–202.
- [14] A.G. Agrios, P. Pichat, J. Photochem. Photobiol. A 180 (2006) 130–135.
- [15] X. Li, J.W. Cabbage, W.S. Jenks, J. Photochem. Photobiol. A 143 (2001) 69–85.
- [16] M. Ranchella, C. Rol, G.V. Sebastiani, J. Chem. Soc., Perkin Trans. 2 (2000) 311–315.
- [17] C. Lang'at-Thoruwa, T. Song Tong, J. Hu, L. Simons Andrian, A. Murphy Patricia, J. Nat. Prod. 66 (2003) 149–151.
- [18] C.G.M. Janssen, E.F. Godefroi, J. Org. Chem. 49 (1984) 3600–3603.
- [19] T.P. Smyth, B.W. Corby, J. Org. Chem. 63 (1998) 8946–8951.
- [20] A.K. Chakraborti, L. Sharma, M.K. Nayak, J. Org. Chem. 67 (2002) 6406–6414.
- [21] C.G. Hatchard, C.A. Parker, Proc. Royal. Soc. A 235 (1956) 518–536.
- [22] W.D. Bowman, J.N. Demas, J. Phys. Chem. 80 (1976) 2434–2435.
- [23] C.C. Sweeley, R. Bentley, M. Makita, W.W. Wells, J. Am. Chem. Soc. 85 (1963) 2497–2507.
- [24] X. Li, J.W. Cabbage, T.A. Tetzlaff, W.S. Jenks, J. Org. Chem. 64 (1999) 8509–8524.
- [25] E. Baciocchi, M. Bietti, O. Lanzalunga, Acc. Chem. Res. 33 (2000) 243–251.
- [26] J. Cunningham, G. Al-Sayyed, S. Srijaranal, in: G.R. Helz (Ed.), Aquatic Surface Photochemistry, Lewis, Boca Raton, FL, 1994, pp. 317–348.
- [27] The surface area of PC 500 is enough greater than the others that it is possible that this catalyst is not fully saturated under our conditions.
- [28] M. Abdulla, G.K.-C. Low, R.W. Matthews, J. Phys. Chem. 94 (1990) 6820–6825.
- [29] K.H. Wang, Y.H. Hsieh, C.H. Wu, C.Y. Chang, Chemosphere 40 (2000) 389–394.
- [30] C. Richard, New J. Chem. 18 (1994) 443–445.
- [31] X. Li, J.W. Cabbage, W.S. Jenks, J. Org. Chem. 64 (1999) 8525–8536.
- [32] J. Cunningham, B.K. Hodnett, J. Chem. Soc. Faraday 1 77 (1981) 2777–2801.
- [33] E. Papaconstantinou, Chem. Rev. 18 (1989) 1–31.
- [34] I.N. Lykakis, C. Tanielian, M. Orfanopoulos, Org. Lett. 5 (2003) 2875–2878.
- [35] X. Li, W.S. Jenks, J. Am. Chem. Soc. 122 (2000) 11864–11870.